Research Square

Preprints are preliminary reports that have not undergone peer review.
They should not be considered conclusive, used to inform clinical practice,
or referenced by the media as validated information.

Development Of A Candidate Biomarker Panel For Tracking Aging-Associated Molecular Changes In A Simplified In Vitro Neural Aging Model

Ceylin Kizilkaya
Black Hills State University
Cade Olson
Black Hills State University
Devin Messer
Black Hills State University
Matthew Pawlus
matthew.pawlus@bhsu.edu

Black Hills State University

Research Article

Keywords: Neural aging, biomarkers, gene expression, in vitro model

Posted Date: November 26th, 2026

DOI: https://doi.org/10.21203/rs.3.rs-11693890/v1

License: This work is licensed under a Creative Commons Attribution 4.0 International License.
Read Full License

Additional Declarations: No competing interests reported.

TITLE:

Development Of A Candidate Biomarker Panel For Tracking Aging-Associated Molecular Changes In A Simplified *In Vitro* Neural Aging Model

AUTHOR INFORMATION:

Ceylin Kizilkaya[1], Cade Olson[1], Devin Messer[1] , Matthew Pawlus (ORCID iD: 0000-0001-6007-7198)[1*]

[1] College of Natural & Behavioral Sciences, Black Hills State University, Spearfish, SD 57799

*Corresponding author; matthew.pawlus@bhsu.edu

1. ABSTRACT

Neural cellular aging involves progressive changes across interconnected biological processes, making its characterization difficult through individual biomarkers. This study aimed to establish a simplified in vitro model of neural cellular aging and determine whether progressive molecular changes within the model could be monitored using a targeted multidimensional panel of aging-related genes. Undifferentiated SH-SY5Y cells were serially passaged without exogenous aging stimuli. Proliferation, intracellular reactive oxygen species (ROS), and senescence-associated β-galactosidase (SA-β-gal) activity were evaluated alongside the expression of eight candidate genes. Linear regression and pathway enrichment analyses were performed to assess passage-dependent expression patterns and their biological relevance. No significant differences were observed in the functional measurements across the passage ranges examined. In contrast, all eight candidate genes exhibited significant passage-dependent expression changes. POT1, E2F2, UBE2C, SUV39H1, YWHAZ, and RPL13A increased with passage number, whereas FOXM1 and COL3A1 decreased. Linear regression demonstrated consistent relationships between gene expression and passage number, with R^2 values ranging from 0.6483 to 0.9645. Pathway enrichment identified associations with interconnected aging-relevant processes, including cellular senescence, cell-cycle regulation, stress responses, telomere homeostasis, and epigenetic regulation. The contrasting expression patterns suggest that molecular changes associated with cellular maintenance and survival may coexist with alterations potentially associated with emerging vulnerabilities, despite the preservation of measured functional characteristics. Together,

these findings support the proposed panel as a candidate approach for monitoring molecular progression across multiple aging-related biological processes.

KEYWORDS:

Neural aging, biomarkers, gene expression, *in vitro* model

STATEMENTS AND DECLARATIONS:

Competing Interests: The authors declare that they have no conflicts of interest with the contents of this article.

ACKNOWLEDGMENTS:

Research reported in this publication was supported by the South Dakota Biomedical Research Infrastructure Network (SD BRIN) through an Institutional Development Award (IDeA) from the National Institute of General Medical Sciences of the National Institutes of Health under grant number P20GM103443. The content is solely the responsibility of the authors and does not necessarily represent the official views of the National Institutes of Health. Cell culturing and functional assays were performed by WestCore at Black Hills State University. The funders had no role in study design, data collection and analysis, decision to publish, or preparation of the manuscript.

2. INTRODUCTION

Biological aging is characterized by the progressive accumulation of structural and functional damage at the cellular, tissue, and organ levels, over time. These alterations contribute to diminished regenerative capacity, impaired cellular homeostasis, and a gradual decline in physiological function (López-Otín vd., 2023). Neural aging is a multifactorial process involving the progressive accumulation of interconnected molecular and cellular alterations within the nervous system, including genomic instability, epigenetic dysregulation, loss of proteostasis, mitochondrial dysfunction, and cellular senescence (Ridderinkhof & Krugers, 2022). Collectively, these alterations contribute to age-associated declines in cognitive functions such as learning, memory, attention, and processing speed (Ridderinkhof & Krugers, 2022). Furthermore, neural aging represents a major risk factor for the development of neurodegenerative disorders, including Alzheimer's disease, and Parkinson's disease (Hou vd., 2019). Although aging does not directly cause neurodegenerative disease, it significantly increases the risk, severity, and rate of progression of these conditions and may also complicate therapeutic intervention (Chou vd., 2023; Hou vd., 2019). Effective therapies for neurodegenerative disorders remain limited, making early detection and intervention particularly important (Hou vd., 2019). The ability to accurately monitor neural aging may improve identification of individuals at increased risk of age-related neurological decline, facilitate earlier intervention strategies, and support the preservation of neural function throughout aging (Jia vd., 2023). A major challenge in monitoring neural aging is the identification and assessment of reliable and specific biomarkers (Jia vd., 2023). Neural aging is a complex process involving coordinated changes across multiple molecular and cellular pathways, many of which are not individually specific to aging (López-Otín vd., 2023; Ridderinkhof & Krugers, 2022). Consequently, no single biomarker is likely to adequately represent the overall process or provide sufficient specificity to attribute an observed change to aging itself (Jia vd., 2023; Ridderinkhof & Krugers, 2022). A panel of diverse biomarkers that show coordinated patterns may therefore provide a more informative means of characterizing neural aging. However, evaluating multiple biomarkers across different biological processes within the already complex aging system would introduce additional sources of variability and would further complicate interpretation. To address this complexity, an experimental strategy designed to simplify the biological system being evaluated while maintaining its relevance and simultaneously broadening the range of biological processes used to assess it is necessary.

With this objective, we first sought to establish an in vitro neural cellular aging model that reflects the fundamental characteristic of biological aging: the progressive accumulation of cellular and molecular alterations over time. SH-SY5Y cells were serially passaged under standard culture conditions without exposure to exogenous aging stimuli, stressors, or other experimental perturbations beyond those required for routine culture maintenance. As passage numbers increase, the cells accumulate greater replicative history and undergo repeated cycles of growth, division, and cellular maintenance, providing a simplified means of modeling the gradual accumulation of alterations that characterizes aging. The same experiments were performed and compared at progressively later passages to determine how the responses changed with cellular aging. The functional experiments that were performed to characterize these initial changes include proliferation, reactive oxygen species (ROS), and senescence-associated β-galactosidase (SA-β-gal). Proliferation reflects the capacity of a cell population to maintain growth and division. Elevated SA-β-gal activity is associated with viable but growth-arrested cells (Hernandez-Segura vd., 2018; Kumari & Jat, 2021). Intracellular ROS levels indicate the degree of oxidative stress experienced by the metabolically active (Davalli vd., 2016; von Zglinicki, 2024). Because these changes are not independently specific to aging, their combined assessment provides a more comprehensive evaluation of the functional state of the cell population and strengthens the interpretation of multifactorial aging-associated cellular changes. SH-SY5Y cell line which are human-derived neuroblastoma cells were particularly chosen for this model because their proliferative capacity (Kovalevich & Langford, 2013) permits repeated passaging and longitudinal assessment across increasing replicative history, while their broad range of neural properties allow these progressive cellular changes to be examined within a neural context (Xicoy vd., 2017), together providing an experimentally tractable system for studying progressive neural cellular aging. SH-SY5Y cells are well characterized and have been widely used to study and model neuronal function, neurodegenerative processes, and neurotoxicity (Kovalevich & Langford, 2013), making the model easily adaptable to additional biological complexity, including adding alternative cellular conditions, neurodegenerative stressors or neuronal differentiation.

After establishing this baseline model of progressive neural cellular aging, a multifactorial candidate biomarker panel was developed to determine whether this progression could be monitored across multiple biological processes. Eight genes were selected based on established roles in biological pathways and cellular processes known to contribute to, or be affected by, aging.

We therefore hypothesized that their expression might also show a measurable relationship with progression through the neural cellular aging model. To our knowledge, these genes have not previously been evaluated together as a coordinated panel in the context of aging. Expression of the selected candidate genes was quantified at progressively later passages to determine whether coordinated expression patterns emerged over time. Linear regression analysis was used to assess the relationship between gene expression and passage number and to determine whether expression patterns were passage dependent. Pathway enrichment analysis was then used to evaluate whether the candidate genes collectively converged on interconnected biological processes relevant to aging. Candidate genes that demonstrated consistent relationships with progression through the model were then considered for inclusion in the proposed neural aging biomarker panel. Taken together, this study aimed to establish a simplified and biologically relevant in vitro model of progressive neural cellular aging and to determine whether aging-associated changes within this model could be characterized using a coordinated, multidimensional biomarker approach. By combining longitudinal functional measurements with candidate gene expression data representing distinct biological processes, the study sought to identify patterns of change that consistently align with increasing cellular age.

3. METHODS

3.1. Cell Culture

Human SH-Sy5Y neuroblastoma cells (ATCC, Manassas, VA, USA) were cultured in Dulbecco's Modified Eagle Medium (DMEM; 2.5 mM L-glutamine, 15 mM HEPES) supplemented with 15% fetal bovine serum (FBS), 1% penicillin-streptomycin, and Amphotericin B. Cells were maintained at 37°C in a humidified atmosphere containing 5% CO_2. All experiments were performed using undifferentiated cells.

3.2. Neural Aging Model

To establish an in vitro model for examining aging-relevant changes during prolonged cellular propagation, SH-Sy5Y neuroblastoma cells were serially passaged from passage 0 (P0; upon receipt from ATCC) through passage 25 (P25) under standard culture conditions. Cells were routinely subcultured upon reaching approximately 85–95% confluency. At selected passages,

cultures were divided so that cells could be collected for experimental analysis while parallel cultures continued through subsequent passages. Passage groups varied among assays according to experimental availability and design. Gene-expression analysis was performed at P2, P5, and P15; intracellular reactive oxygen species were measured at P2, P6, and P15; senescence-associated β-galactosidase activity was measured at P2, P6, P15, and P25; and proliferation was assessed at P15, P18, and P22. No experimental treatments or manipulations were performed during serial propagation beyond routine culture maintenance and subculturing.

3.3. Intracellular Reactive Oxygen Species (ROS)

SH-Sy5Y cells were seeded at a density of 135,000 cells per well in 12-well plates and allowed to adhere for 24 h under standard culture conditions. Culture medium was then replaced, and cells were incubated for an additional 24 h prior to assay initiation. Intracellular ROS levels were quantified using a DCFH-DA fluorometric assay kit (Novus Biologicals) according to the manufacturer's instructions. Cells were incubated with DCFH-DA (20 µM) for 1 h at 37 °C protected from light. Following incubation, cells from each well were transferred in equal volumes into three technical replicate wells of a 96-well plate. Fluorescence was measured immediately using a microplate reader with excitation at 500 nm and emission at 525 nm. Experiments were performed using three biological replicates.

3.4. Senescence-Associated β-Galactosidase

SH-Sy5Y cells were seeded at a density of 135,000 cells per well in 12-well plates and allowed to adhere for 24 h under standard culture conditions. Culture medium was then replaced, and cells were incubated for an additional 24 h prior to assay initiation. Senescence-associated β-galactosidase (SA-β-gal) activity was quantified using the Mammalian β-Galactosidase Assay Kit (Thermo Fisher Scientific) following the manufacturer's protocol (Adherent Cells, Method 1). Cells were washed once with phosphate-buffered saline (PBS; pH 7.2), and 350 µL of β-galactosidase assay reagent was added directly to each well. Plates were incubated for 30 min at 37 °C, after which the reaction was terminated by the addition of 200 µL of β-galactosidase assay stop solution. Samples from each well were then distributed equally into four technical replicate wells of a 96-well plate. Absorbance was measured at 405 nm using a microplate reader. Experiments were performed using three biological replicates.

3.5. Proliferation

SH-Sy5Y cells were seeded in 96-well plates at a density of 10,000 cells per well and maintained under standard culture conditions for 48 h prior to analysis. Cell proliferation was assessed using the FastCount Cell Proliferation Assay Kit (MP Biomedicals) according to the manufacturer's instructions. Briefly, 20 µL of FastCount reagent was added directly to each well containing 100 µL of culture medium. Cells were incubated for 3 h under standard culture conditions, after which absorbance was measured at 555 nm using a microplate reader. Experiments were performed using three biological replicates, with each biological replicate analyzed in a minimum of three technical replicates.

3.6. RNA Isolation and cDNA Synthesis

Total RNA was isolated from SH-Sy5Y cells using the GeneJET RNA Purification Kit (Thermo Fisher Scientific) according to the manufacturer's protocol for mammalian cultured cells. RNA concentration and purity were determined using a spectrophotometer. Subsequently, 500 ng of total RNA was reverse transcribed into complementary DNA (cDNA) using the RevertAid First Strand cDNA Synthesis Kit (Thermo Fisher Scientific) according to the manufacturer's instructions.

3.7. qPCR

Expression of eight specific genes was quantified by SYBR Green-based quantitative real-time PCR (qPCR) using Qiagen SYBR Green Master Mix and cDNA synthesized as described above. Reactions were performed in triplicate with a final reaction volume of 20 µL using three independent biological replicates. Relative gene expression was determined using the comparative threshold cycle (ΔΔCt) method and normalized to *HPRT1*, which served as the endogenous reference gene. *HPRT1* expression remained stable across the passage groups examined. Primer specificity was verified by melt curve analysis, and amplification efficiencies were assessed by standard curve analysis. All primer sets demonstrated amplification efficiencies between 86% and 110%. Primer sequences, annealing temperatures, and amplification efficiencies are provided in Supplementary Table S1.

3.8. Pathway Enrichment Analysis

To investigate the biological processes associated with the candidate neural aging biomarkers evaluated by qPCR, pathway enrichment analysis was performed using Enrichr (Kuleshov vd., 2016). The eight candidate genes showing significant passage-dependent expression changes were submitted as a gene list for enrichment analysis. Functional enrichment was assessed using the Reactome Pathways 2024 and Elsevier Pathway Collection libraries available through Enrichr. Statistical significance was assessed using adjusted p-values calculated with the Benjamini–Hochberg false discovery rate (FDR) correction to account for multiple hypothesis testing. Pathways with an adjusted $p < 0.05$ were considered statistically significant. The identified pathways were subsequently grouped according to their primary biological functions to facilitate interpretation of the aging-relevant cellular processes represented by the candidate panel.

3.9. Statistical Analysis

Statistical analyses were performed using Microsoft Excel and GraphPad Prism (GraphPad Software, Boston, MA, USA). Raw data were processed and relative gene expression values were calculated in Microsoft Excel prior to statistical analysis and figure generation in GraphPad Prism. Data are presented as mean ± standard deviation (SD), unless otherwise stated. For proliferation, intracellular reactive oxygen species (ROS), and senescence-associated β-galactosidase activity assays, differences among passage groups were analyzed using one-way analysis of variance (ANOVA) followed by Tukey's multiple-comparisons test. For qPCR assays, relative gene expression was calculated using the ΔΔCt method, normalized to *HPRT1*, and analyzed across passage groups using one-way ANOVA followed by Tukey's multiple-comparisons test. The relationship between gene expression and passage number was evaluated by linear regression analysis, and the coefficient of determination (R^2) was used to assess the consistency of expression changes associated with passage number. Statistical significance was defined as $p < 0.05$. Significance levels are indicated as $*p < 0.05$, $**p < 0.01$, $***p < 0.001$, and $****p < 0.0001$.

4. RESULTS

4.1. Functional Characterization of the Neural Aging Model

An in vitro neural aging model was established through serial passaging of SH-Sy5Y cells. Serial passaging exposes cells to repeated cycles of growth and division over time. Cells from earlier and later passages were used to represent younger and older cell populations within the neural aging model. To characterize the functional phenotype of neural aging at the cellular level, cell proliferation, intracellular reactive oxygen species (ROS) production, and β-galactosidase (β-gal) activity were evaluated. No significant differences were observed in any of the three functional measurements as cellular age increased (Figure 1). Cells at later passages therefore exhibited functional characteristics comparable to those observed at earlier passages.

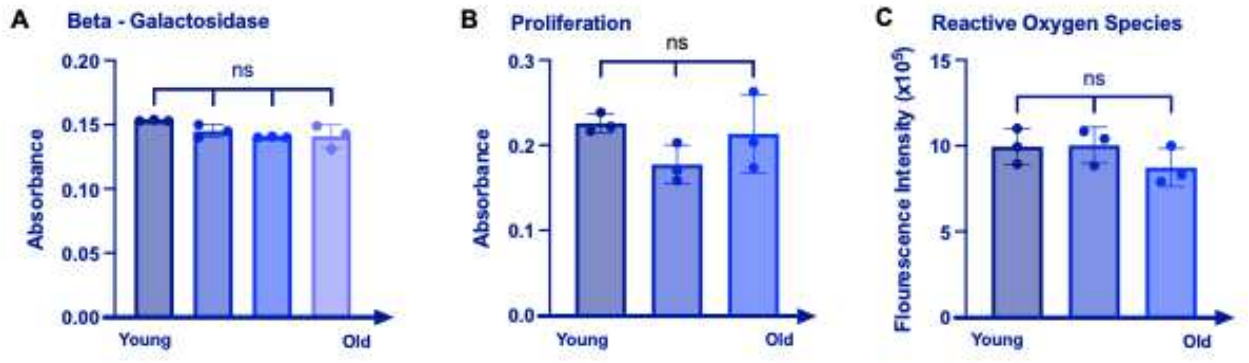


Figure 1. ROS, proliferation, and SA-β-gal activity in younger and older SH-Sy5Y cells within the neural aging model. (A) Senescence-associated β-galactosidase (SA-β-gal) activity was measured at P2, P6, P15, and P25. (B) Cell proliferation was measured at P15, P18, and P22. (C) Intracellular reactive oxygen species (ROS) levels were measured at P2, P6, and P15. Passage groups are presented in increasing order within each assay. Data are presented as mean ± SD from three independent biological replicates (n = 3). Statistical analysis was performed separately for each functional endpoint using one-way ANOVA followed by Tukey's multiple-comparisons test. No significant differences were detected among the passage groups examined within any of the three functional assays.

4.2. Expression Profiling of Candidate Neural Aging Biomarkers

Candidate genes associated with aging-related cellular processes were selected based on literature review and their established roles in pathways implicated in neural aging. Relative gene expression was quantified across P2, P5, and P15 cells and normalized to the endogenous reference gene HPRT1. Significant passage-dependent expression changes were observed across the candidate panel. Expression of *POT1*, *E2F2*, *UBE2C*, *SUV39H1*, *YWHAZ*, and *RPL13A* increased significantly with cellular age, whereas *FOXM1* and *COL3A1* expression decreased significantly (Figure 2). Linear regression analysis was performed to evaluate the relationship between gene expression and passage number and to determine the consistency of the observed expression trends across progressively older cells. Linear regression analysis demonstrated corresponding passage-dependent trends for all eight genes, with coefficients of determination ranging from $R^2 = 0.6483$ to $R^2 = 0.9645$ (Figure 3).

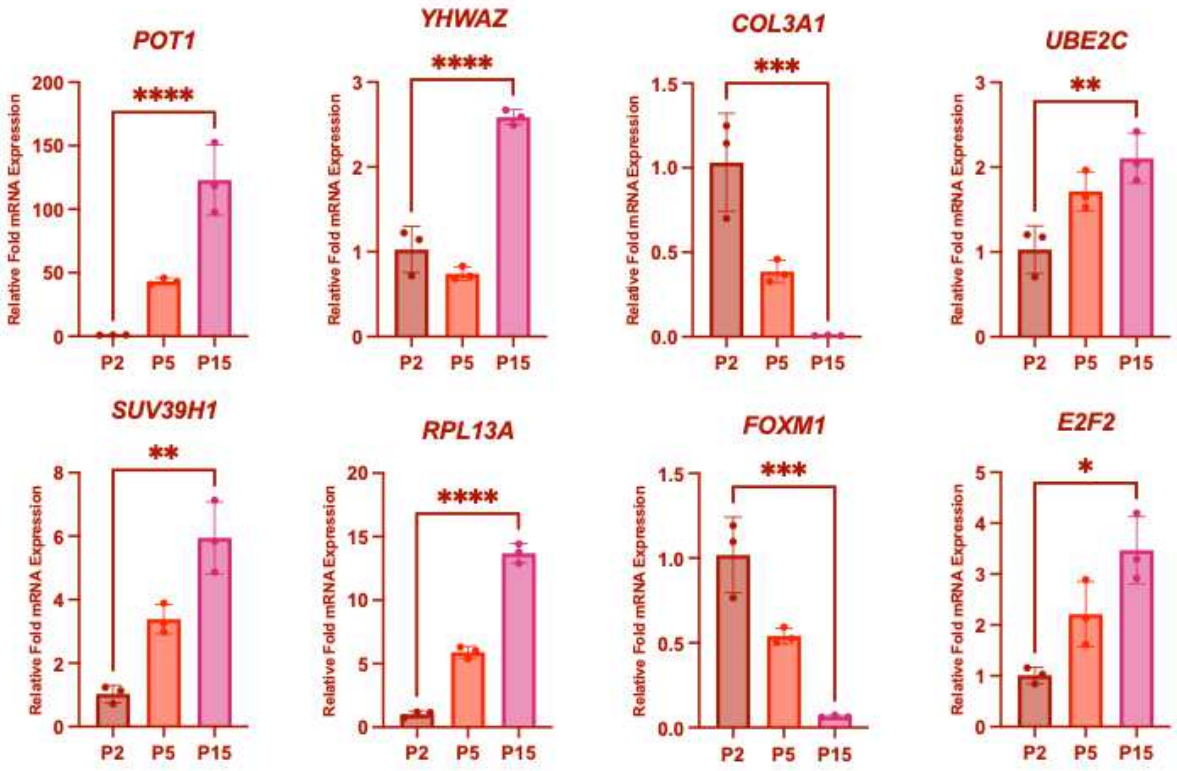


Figure 2. Expression of candidate neural aging biomarkers in the SH-Sy5Y neural aging model. Relative expression of the candidate genes was quantified by qPCR in P2, P5, and P15 SH-Sy5Y cells and normalized to HPRT1 using the ΔΔCt method. Data are presented as mean ± SD

from three independent biological replicates (n=3), as indicated for each gene. Statistical significance was determined using one-way ANOVA followed by Tukey's multiple-comparisons test. Significance levels are indicated as *p < 0.05, **p < 0.01, ***p < 0.001, and ****p < 0.0001.

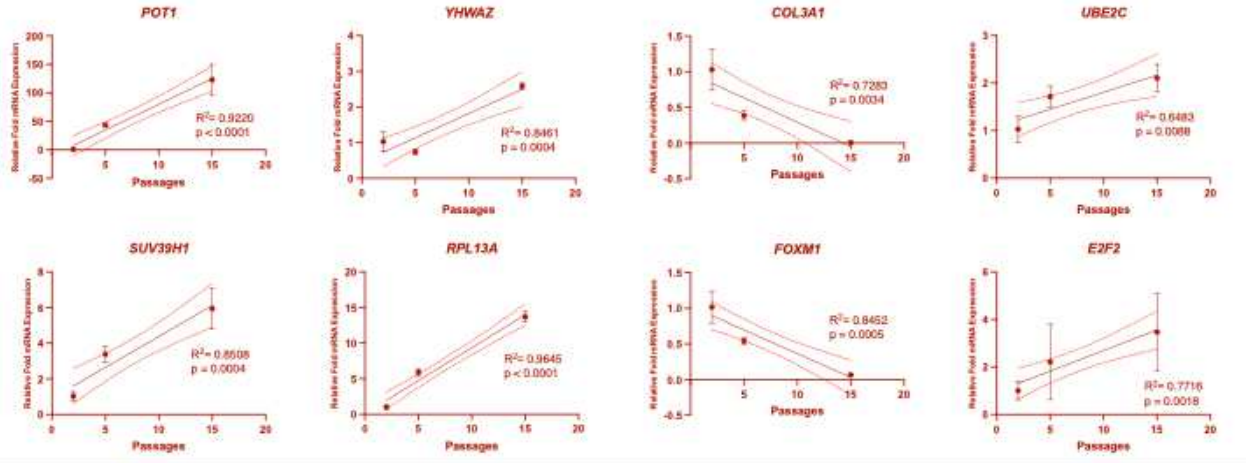


Figure 3. Linear regression analysis of candidate neural aging biomarker expression in the SH-Sy5Y neural aging model. Relative expression of each candidate gene was evaluated as a function of passage number. Data points are presented as mean ± SD from three biological replicates at each passage. Linear regression was performed using the relative gene-expression values from individual biological replicates. Solid lines represent the fitted linear-regression models, and dashed lines represent the corresponding 95% confidence bands. The coefficient of determination (R^2) is shown for each gene.

4.3. Functional Pathway Enrichment Analysis of Candidate Neural Aging Biomarkers

To further characterize the biological pathways represented by the selected candidate genes associated with aging-related cellular processes, pathway enrichment analysis was performed using the Reactome and Elsevier pathway databases. Reactome pathway enrichment analysis identified significant enrichment of pathways involved in cellular senescence, cell cycle regulation, mitotic cell cycle, and cellular responses to stress (Table 1). Elsevier pathway enrichment analysis similarly identified enrichment of pathways related to telomere homeostasis, aging, epigenetic regulation, proliferative signaling, cell cycle regulation, cellular senescence, and cell survival (Table 2).

Reactome Pathways	Adjusted p-value
Cellular Senescence	0.003713
Cell Cycle	0.003713
Aberrant Regulation of Mitotic Cell Cycle Due to RB1 Defects	0.003713
Diseases of Mitotic Cell Cycle	0.003713
Cellular Responses to Stress	0.00446
Cellular Responses to Stimuli	0.005905
Cell Cycle, Mitotic	0.01885

Table 1. Reactome pathway enrichment analysis of candidate neural aging biomarker panel.

Elsevier Pathway Collection		Adjusted p-value
Telomere Homeostasis	Telomer Attrition Triggers Genomic Instability	0.02384
	Telomere Maintenance	0.02318
Aging	Extracellular Matrix Degradation in Skin Aging	0.02154
	Proteins Involved in Stem Cell Exhaustion in Aging	0.02384
	Proteins Involved in Hutchinson-Gilford Progeria Sindrome	0.02154
Epigenetic Regulation	Proteins with Altered Expression in Cancer-Associated Histone Methylation	0.02154
	Epigenetic Alterations Triggers Genomic Instability	0.02154
	Histone Methylation	0.02318
Sustained Proliferation	Proteins with Altered Expression in Cancer-Associated Sustaining of Proliferative Signaling	0.02154
	Genes with Mutations in Cancer-Associated Sustaining of Proliferative Signaling	0.04943
Cell Cycle Regulation	G2/M Phase Transition	0.02318
	G1/S Phase Transition	0.02318
Cellular Senescene	Oncogene Induced Cellular Senescence	0.02629
Cell Survival	DDR1 -> NF-kB Signaling	0.02154

Table 2. Elsevier pathway enrichment analysis of candidate neural aging biomarker panel.

5. DISCUSSION

5.1. Functional Stability During the Neural Aging Model

The present study used serial passaging of SH-Sy5Y cells to model the gradual accumulation of aging-associated cellular changes during repeated growth and propagation in the absence of acute exogenous stressors. Passage number was used as an operational measure of cellular age and

cumulative replicative history. Within this framework, proliferation, intracellular reactive oxygen species (ROS), and senescence-associated β-galactosidase (SA-β-gal) activity were evaluated together to provide functional context for the aging-related changes tracked in the model. These measurements provide complementary information regarding cellular growth capacity, oxidative stress, and senescence-associated alterations and therefore allow the functional state of the cell population to be assessed more comprehensively than any individual endpoint alone (Hernandez-Segura vd., 2018; López-Otín vd., 2023). The extended proliferative lifespan of SH-Sy5Y cells was expected to provide a broader experimental window in which gradual aging-associated changes could be observed while cellular function remained measurable. However, no significant differences in proliferation, ROS levels, or SA-β-gal activity were observed as the passages progressed. These findings indicate that within this model, increasing cellular age was not accompanied by detectable impairment of proliferation, increased basal oxidative stress, or accumulation of a senescence-associated phenotype.

The maintenance of functional stability may have several explanations, including the intrinsic resilience of the SH-Sy5Y cell line and progressive adaptation or selection during routine culture. As an immortalized neuroblastoma-derived cell line, SH-Sy5Y cells possess sustained proliferative capacity and greater tolerance for repeated propagation than finite neural cell populations (Kovalevich & Langford, 2013). Previous long-term cultivation of undifferentiated SH-Sy5Y cells demonstrated stable cumulative population doubling across approximately 12 consecutive passages, supporting the sustained proliferative capacity of this cell line during extended culture (Feles vd., 2022). The present study extended this characterization to later experimental stages, reaching P22 for proliferation and P25 for SA-β-gal analysis. Despite this broader passage range, proliferation, intracellular ROS levels, and SA-β-gal activity remained stable across the cellular ages examined. These findings extend previous observations of proliferative stability by demonstrating that undifferentiated SH-Sy5Y cells may also maintain basal intracellular ROS levels and SA-β-gal activity during continued neural cellular aging. However, immortalization does not make the cells indefinitely resistant to aging-associated cellular changes. Thus, the cells may have continued to undergo aging-related molecular and regulatory changes while remaining comparatively resistant to overt functional deterioration within the passage range examined.

A second, non-mutually exclusive explanation involves the effects of routine culture maintenance on the composition of the cell population. SH-Sy5Y cells normally grow and proliferate as an adherent population, although the presence of a smaller non-adherent fraction in the culture medium is a routine feature of cell culture. Cells may become temporarily detached because of normal population turnover or transient changes in adhesion; however, the non-adherent fraction may also include cells with reduced viability, impaired adhesion-related function, increased sensitivity to cellular stress, or ongoing cell death. During routine medium replacement, adherent cells generally remain attached to the culture surface, whereas non-adherent cells are removed with the spent medium. Although this process ordinarily supports the maintenance of a viable and experimentally suitable culture, its repeated occurrence throughout the present study may have gradually reduced the representation of cells with weaker attachment or lower stress tolerance. In addition, only cells capable of tolerating repeated detachment, transfer, reattachment, and continued proliferation contributed effectively to subsequent passages. Together, the intrinsic properties of SH-Sy5Y cells and the cumulative effects of routine culture procedures may therefore have progressively enriched the population for cells with greater adhesive, proliferative, and functional resilience. Such culture-associated selection could have contributed to the maintenance of proliferation, intracellular ROS levels, and SA-β-gal activity as cellular age increased. Although changes in population composition were not directly assessed, this mechanism provides a plausible explanation for the stable functional phenotype observed in the model.

Importantly, the absence of detectable changes in proliferation, intracellular ROS levels, and SA-β-gal activity does not negate the substantial cumulative culture history acquired by the cells over serial passage. Although culture-associated selection or the sustained proliferative capacity of SH-SY5Y cells may have contributed to the preservation of these functional characteristics, cells at later passages had nevertheless undergone repeated cycles of growth, division, and cellular maintenance over an extended period, representing a markedly greater cumulative culture and replicative history than cells at earlier passages.

5.2. Candidate Biomarker Selection

Cellular aging is a multifactorial process that cannot be adequately characterized through a single molecular marker (Jia vd., 2023; López-Otín vd., 2023). Therefore, eight initial candidate genes

were selected to create a multifactorial candidate-biomarker panel based on their established associations with distinct biological processes relevant to aging. Each candidate was selected to represent a different aspect of cellular aging, allowing progression through the serial-passage model to be evaluated across multiple molecular processes rather than through a single biological readout.

5.2.1. POT1

Telomere dysfunction and loss of genome stability are established features of aging (López-Otín vd., 2023). POT1 is a component of the shelterin complex that protects telomeric chromosome ends and supports telomere replication and length regulation (Zade & Khattar, 2023). Disruption or reduced expression of *POT1* has previously been associated with telomere dysfunction, replication stress, DNA-damage signaling, chromosomal instability, and proliferative arrest (Kondo vd., 2004; Pinzaru vd., 2016; Takai vd., 2016). Furthermore, increased *POT1* expression has been observed following stress- and inflammation-associated signaling (Butler vd., 2012) and during adaptation to sustained immune-mediated selection (Carré vd., 2021), suggesting that *POT1* regulation can increase under prolonged cellular demand. Taken together, *POT1* was hypothesized to represent changes in telomere maintenance and genome stability in the neural cellular aging model and was therefore selected for inclusion in the candidate biomarker panel.

5.2.2. SUV39H1

Epigenetic regulation and chromatin organization progressively decline with cellular aging, while senescence-associated processes become increasingly prominent (López-Otín vd., 2023). Although these processes are distinct, they are biologically interconnected and can influence one another during aging. SUV39H1 supports genome stability through H3K9 trimethylation and the maintenance of constitutive heterochromatin. Loss of SUV39H-dependent regulation disrupts heterochromatin organization and increases chromosomal instability, linking this epigenetic mechanism to the preservation of chromatin integrity (Peters vd., 2001). On the other hand, declining *SUV39H1* expression has been associated with reduced H3K9me3, loss of transcriptional silencing, as well as replicative senescence (Sidler vd., 2014). Restoration or increased expression of *SUV39H1* has been shown to support cell-cycle activity (Sidler vd., 2014) and reduce selected senescence-associated inflammatory signals (Li vd., 2023). Taken together, *SUV39H1* was

hypothesized to represent changes in epigenetic regulation, chromatin stability, and senescence-associated processes in the neural cellular aging model and was therefore selected for inclusion in the candidate biomarker panel.

5.2.3. E2F2

Cell-cycle regulation is progressively altered during cellular aging (López-Otín vd., 2023). One important factor affecting cell-cycle regulation is the accumulation of DNA damage and disruptions in DNA metabolism, which can interfere with normal cell-cycle progression (Yates vd., 2025). E2F2 contributes to the transcriptional coordination of DNA metabolism and cell-cycle regulation, targeting genes involved in DNA replication, DNA damage responses, and cell-cycle progression (Laresgoiti vd., 2013). Experimental manipulation of *E2F2* expression demonstrated a directional relationship with cellular function, with lower expression associated with increased DNA damage, cell-cycle arrest, and reduced proliferation and higher expression associated with reduced DNA damage, decreased cell-cycle arrest, and improved proliferative function (Liu vd., 2022). Taken together, *E2F2* was hypothesized to represent changes in cell-cycle regulation in relation to DNA metabolism and replicative maintenance in the neural cellular aging model and was therefore selected for inclusion in the candidate biomarker panel.

5.2.4. UBE2C

Ubiquitin-mediated protein regulation is altered during cellular aging, contributing to disruptions in protein turnover and cellular homeostasis (Hamazaki & Murata, 2024). UBE2C is an E2 ubiquitin-conjugating enzyme that facilitates the ubiquitination and proteasomal degradation of target proteins, most notably through its interaction with the anaphase-promoting complex/cyclosome. Reduced *UBE2C* expression has been shown to decrease p53 ubiquitination and degradation, impair cell-cycle progression, and reduce proliferation (Huang & Li, 2024) Increased *UBE2C* expression, on the other hand, promotes ubiquitin-dependent degradation of regulatory proteins and has been associated with sustained cell-cycle progression and cellular proliferation (Chiang vd., 2021; Huang & Li, 2024; Kim vd., 2020). Taken together, *UBE2C* was hypothesized to represent changes in ubiquitin-mediated protein regulation and turnover in the neural cellular aging model and was therefore selected for inclusion in the candidate biomarker panel.

5.2.5. FOXM1

Cell-cycle progression and mitotic function become increasingly impaired during cellular aging. FOXM1 is a transcription factor that coordinates the expression of genes required for G2/M progression and mitosis, including genes involved in chromosome segregation, spindle function, and cytokinesis (Laoukili vd., 2005, 2007). Decreased *FOXM1* expression during cellular aging has been associated with prolonged mitosis, chromosome mis-segregation, aneuploidy, and progression toward senescence (Macedo vd., 2018). Increased *FOXM1* expression in aged cells has been shown to restore mitotic function, reduce chromosome segregation errors, and ameliorate senescence-associated phenotypes (Macedo vd., 2018). Taken together, *FOXM1* was hypothesized to represent changes in cell-cycle progression, mitotic regulation, and chromosomal stability in the neural cellular aging model and was therefore selected for inclusion in the candidate biomarker panel.

5.2.6. YWHAZ

Cellular aging is accompanied by increasing demands on signaling pathways that regulate stress responses, survival, and maintenance of cellular function (Haigis & Yankner, 2010; Wu vd., 2024). YWHAZ encodes the 14-3-3ζ signaling adaptor, which regulates the stability, activity, and localization of phosphorylated proteins involved in signal transduction, apoptosis, autophagy, cell-cycle regulation, and cellular survival (Gan vd., 2020). Reduced *YWHAZ* expression has been associated with decreased proliferation and greater susceptibility to apoptosis, indicating that loss of 14-3-3ζ signaling can impair cellular growth and survival responses (Nishimura vd., 2013; Wang vd., 2017). Increased *YWHAZ* expression has been associated with enhanced proliferative capacity and resistance to apoptosis, supporting a role for 14-3-3ζ in maintaining cellular viability under sustained challenge (Nishimura vd., 2013). Taken together, *YWHAZ* was hypothesized to represent changes in stress-response and survival signaling in the neural cellular aging model and was therefore selected for inclusion in the candidate biomarker panel.

5.2.7. RPL13A

Translational regulation and protein production undergo age-associated changes across diverse cell types and tissues (Anisimova vd., 2020). RPL13A is a component of the 60S ribosomal subunit

that contributes to protein synthesis and also performs an extraribosomal role in selective translational control (Mazumder vd., 2003). Experimental depletion or loss of RPL13A disrupts this selective translational repression, leading to increased translation of inflammatory target mRNAs and impaired resolution of inflammatory responses without broadly suppressing protein synthesis (Basu vd., 2014; Poddar vd., 2013). In human bone marrow, *RPL13A* was identified as the most conserved age-associated differentially expressed gene across 17 cell types, with expression increasing with donor age (Lee vd., 2023). Similarly, *RPL13A* was found to increase with age across nearly all tissue–cell types examined in mice, where its upregulation was discussed in the context of its role in limiting inflammatory protein expression and supporting the resolution of inflammatory responses (Zhang vd., 2021). Although *RPL13A* is commonly used as a housekeeping or reference gene in some experimental systems, its reported age-associated expression patterns suggested that it may also be informative in the context of neural cellular aging and was therefore selected for inclusion in the candidate biomarker panel.

5.2.8. COL3A1

Extracellular-matrix homeostasis progressively deteriorates during aging, with age-associated changes in collagen synthesis, organization, and turnover altering tissue structure and cellular function (Birch, 2018; Statzer vd., 2023). *COL3A1* encodes the α1 chain of type III collagen, a major fibrillar component of the extracellular matrix that provides structural support and contributes to tissue strength and organization (Kuivaniemi & Tromp, 2019). Experimental reduction of *COL3A1* has been shown to impair cellular growth, colony formation and migration, demonstrating that its function extends beyond structural support to the regulation of cellular activity (Gao vd., 2018). Reduced COL3A1 expression and type III collagen production have been observed in aging- and senescence-associated models (Rong vd., 2019). Taken together, *COL3A1* was hypothesized to represent changes in extracellular-matrix regulation and remodeling during progression through the neural cellular aging model and was therefore selected for inclusion in the candidate biomarker panel.

5.3. Passage-Dependent Expression of Candidate Neural Aging Biomarkers

The candidate-gene analysis provided two complementary measures of molecular progression through the neural cellular aging model: changes in gene expression across progressively later

passages and the strength of the relationship between expression and passage number. All eight candidate genes exhibited significant passage-dependent expression changes, demonstrating that the cells underwent measurable molecular alterations despite the preservation of proliferation, intracellular ROS levels, and SA-β-gal activity within the passage ranges examined. POT1, E2F2, UBE2C, SUV39H1, YWHAZ, and RPL13A expression increased with passage number, whereas FOXM1 and COL3A1 expression decreased. These opposing patterns indicate that continued serial propagation was accompanied by selective changes in gene expression rather than a uniform transcriptional response across the aging-relevant processes represented by the panel.

As the cells accumulated greater replicative history, increased POT1 expression may be consistent with increased demands on telomere protection and replication-associated maintenance, while increased SUV39H1 expression may reflect continued regulation of heterochromatin organization and epigenetic mechanisms associated with genome stability. These changes occurred alongside increased E2F2 expression, which may indicate continued transcriptional regulation of DNA replication, DNA-damage responses, and cell-cycle progression, while increased UBE2C expression may reflect sustained regulation of ubiquitin-mediated degradation of proteins involved in mitotic progression. The increase in YWHAZ may similarly be consistent with greater involvement of survival-associated signaling in maintaining cellular viability, whereas increased RPL13A expression may reflect changes in translational regulation, including mechanisms involved in controlling inflammatory protein expression. Notably, the expression of these genes became progressively higher as passage number increased and the cells accumulated greater replicative history, potentially accompanied by increasing aging-associated demands. When considered alongside previous findings, the biological effects associated with increased expression of these genes appear to counteract cellular alterations commonly associated with aging. Together, these observations raise the possibility that their progressive upregulation represents a maintenance- or adaptation-associated response to the increasing demands of cellular aging, potentially contributing to the preservation of the measured functional phenotype. However, as these genes increased, FOXM1 expression declined, suggesting a potentially contrasting change in the regulation of mitotic progression, chromosome segregation, and mitotic fidelity. This decrease is particularly relevant because continued proliferation does not necessarily indicate that the molecular regulation of accurate cell division remains unchanged. Similarly, declining COL3A1 expression may reflect changes in extracellular-matrix regulation and maintenance,

potentially indicating alterations in cell–matrix interactions during prolonged propagation. When considered together, these opposing expression patterns suggest that molecular changes consistent with continued cellular maintenance and proliferative regulation may coexist with alterations potentially associated with emerging vulnerabilities in mitotic and extracellular-matrix regulation.

Linear regression analysis demonstrated that changes in the expression of all eight candidate genes were strongly associated with increasing passage number, with R^2 values ranging from 0.6483 to 0.9645, including five of the eight genes exhibiting R^2 values above 0.84. Linear regression was particularly important to the goal of the present study because identifying significant differences in gene expression between passage groups alone was not sufficient to determine how consistently those changes tracked increasing cellular age. By demonstrating strong relationships between expression and passage number, the regression analysis provided additional evidence that the candidate genes could be used to monitor molecular progression through the model. Higher R^2 values indicated stronger linear relationships between gene expression and passage number, suggesting that genes with higher values may be more promising in terms of consistently tracking or predicting molecular progression. Conversely, genes with comparatively lower R^2 values exhibited weaker but still significant linear relationships. The present study aimed to develop a coordinated panel capable of capturing a consistent, multidimensional pattern of molecular changes across different aging-relevant biological processes rather than relying on an individual marker. Within this framework, genes with comparatively lower R^2 values may still be useful components of the initial panel because they represent additional biological processes relevant to neural cellular aging. As the panel undergoes further validation, its composition can be refined by retaining the most informative candidates, removing or replacing less informative genes, or incorporating additional markers that strengthen its ability to track molecular progression.

Taken together, the gene-expression and linear-regression analyses demonstrated that all eight initially selected candidate genes exhibited significant and consistent relationships with progression through the neural cellular aging model. Although the strength of these relationships varied among candidates, their passage-dependent expression patterns support their potential as components of a multidimensional biomarker panel. These molecular changes were detectable despite the absence of significant differences in proliferation, intracellular ROS levels, and SA-β-gal activity within the passage ranges examined, highlighting the potential of the panel to track

molecular progression and potentially identify changes before they become apparent through functional measurements. When interpreted in the context of the previously established biological roles of these genes, the observed expression patterns are consistent with molecular changes associated with cellular maintenance, adaptation, and emerging aging-associated vulnerabilities during continued propagation. Although the panel does not capture every molecular process involved in aging, it provides an integrated framework for following the emerging cellular trajectory. Corresponding changes in protein activity and downstream cellular processes were not yet directly evaluated in the present model however the findings still provide strong evidence supporting all eight initially selected genes as potential components of the biomarker panel and establish a foundation for their further validation.

5.4. Pathway Enrichment Reveals Convergence on Aging-Related Cellular Processes

Pathway-enrichment analysis was performed to determine whether the candidate genes represented interconnected biological processes relevant to progression through the neural aging model. Unlike the preceding gene-expression and linear-regression analyses, pathway enrichment did not evaluate the direction, magnitude, or passage-dependent pattern of gene expression. Instead, it assessed whether the genes included in the candidate panel were represented within shared biological pathways more frequently than expected by chance. The Reactome and Elsevier analyses identified significant enrichment across multiple aging-relevant cellular processes. All pathways presented in Tables 1 and 2 remained significant following correction for multiple comparisons, with adjusted *p*-values ranging from 0.003713 to 0.01885 in the Reactome analysis and from 0.02154 to 0.04943 in the Elsevier analysis. The Reactome analysis showed convergence on cellular senescence, cell-cycle regulation, mitotic regulation, and cellular responses to stress and stimuli. The Elsevier analysis expanded this functional context by identifying enrichment of pathways related to telomere homeostasis, genomic instability, aging, epigenetic regulation, sustained proliferative signaling, cell-cycle transitions, cellular senescence, and cell survival. The recurrence of cell-cycle- and senescence-associated categories across both databases supports the functional coherence of the candidate panel and indicates that the selected genes are associated with overlapping regulatory systems relevant to continued proliferation, cellular maintenance, stress responsiveness, and aging-associated change. The enrichment analysis therefore provided an additional level of organization to the findings by showing that these genes were not

functionally isolated markers but components of interconnected aging-relevant biological systems. The convergence across two pathway databases supports the biological coherence of the panel and strengthens its interpretation as an integrated framework for examining molecular changes associated with cellular aging, maintenance, and adaptation during prolonged propagation.

5.5. Future Directions

The present study demonstrated that all eight candidate genes exhibited significant passage-dependent expression changes in the absence of exogenous aging stimuli. Future studies could investigate whether these expression patterns are also observed when aging-associated cellular changes are induced through experimental stressors. The expression of the candidate genes and the functional experiments could be evaluated following stress-induced aging and compared with the patterns observed during extended serial passaging. These comparisons would provide further evidence to support the biological aging relevance of the model. Afterwards the candidate panel could also be expanded to include genes more directly associated with neurodegenerative diseases, this would increase its potential relevance to disease-associated neural aging. Further studies could evaluate the panel in differentiated SH-SY5Y cells and other neural cell models to determine whether the observed expression patterns are reproducible across different cellular systems. Together, these approaches would support the continued refinement and validation of the proposed biomarker panel and help establish its potential utility for monitoring aging-associated molecular changes in increasingly physiologically relevant neural models.

Although these proposed directions reflect the research interests of the present study, the model and candidate panel are not limited to these applications. They could also be incorporated into existing studies investigating different treatments, diseases, genetic mutations, or biological pathways. By examining an additional variable alongside the established passage-dependent expression patterns, researchers could determine whether their variable of interest is associated with changes in aging-relevant molecular processes. This approach may reveal previously unexamined associations and help guide further research into the involvement of different biological processes in aging.

6. CONCLUSION

The present study addressed the challenge of characterizing neural cellular aging as a multifactorial process by combining a simplified experimental model with a multidimensional biomarker approach. Prolonged serial passaging of undifferentiated SH-SY5Y cells provided a means of examining responses to increasing replicative history without introducing exogenous aging stimuli. Although proliferation, intracellular ROS levels, and SA-β-gal activity remained unchanged across the passage examined, all eight candidate genes exhibited significant and consistent passage-dependent expression changes. Expression patterns observed among the candidate genes suggest that continued cellular maintenance, proliferative regulation, and survival-associated responses coexist with alterations potentially associated with emerging vulnerabilities in mitotic and extracellular-matrix regulation, throughout prolonged passaging within the model. These findings demonstrate that continued cellular propagation was accompanied by consistent trend of molecular alterations despite the preservation of the measured functional characteristics. The consistent relationships between gene expression changes and increased passage number support the potential of the candidate panel in tracking molecular progression through the model. Pathway enrichment further supports that the selected genes represent interconnected biological processes relevant to aging. Together, these findings demonstrate the value of a multidimensional biomarker panel in characterizing cellular changes associated with aging. Rather than relying solely on indicators of functional decline, the proposed approach allows molecular progression to be examined in the context of the cellular response, including the maintenance of functional stability. Although the specificity of these molecular changes to biological aging remains to be established, this study identifies an initial eight-gene candidate panel for monitoring molecular progression over time in a neural cellular model. More broadly, it provides a foundation for investigating how interconnected aging-associated molecular processes relate to cellular maintenance, adaptation, and functional deterioration, contributing to the long-term objective of understanding and monitoring the cellular changes underlying neural aging and age-related neurological decline.

7. REFERENCES

Anisimova, A. S., Meerson, M. B., Gerashchenko, M. V., Kulakovskiy, I. V., Dmitriev, S. E., & Gladyshev, V. N. (2020). Multifaceted deregulation of gene expression and protein synthesis with age. *Proceedings of the National Academy of Sciences*, *117*(27), 15581-15590. https://doi.org/10.1073/pnas.2001788117

Basu, A., Poddar, D., Robinet, P., Smith, J. D., Febbraio, M., Baldwin, W. M., & Mazumder, B. (2014). Ribosomal Protein L13a Deficiency in Macrophages Promotes Atherosclerosis by Limiting Translation Control-Dependent Retardation of Inflammation. *Arteriosclerosis, thrombosis, and vascular biology*, *34*(3), 533-542. https://doi.org/10.1161/ATVBAHA.113.302573

Birch, H. L. (2018). Extracellular Matrix and Ageing. Içinde J. R. Harris & V. I. Korolchuk (Ed.), *Biochemistry and Cell Biology of Ageing: Part I Biomedical Science* (ss. 169-190). Springer. https://doi.org/10.1007/978-981-13-2835-0_7

Butler, K. S., Hines, W. C., Heaphy, C. M., & Griffith, J. K. (2012). Coordinate regulation between expression levels of telomere-binding proteins and telomere length in breast carcinomas. *Cancer Medicine*, *1*(2), 165-175. https://doi.org/10.1002/cam4.14

Carré, T., Thiery, J., Janji, B., Terry, S., Gros, G., Meurice, G., Kieda, C., Olive, D., & Chouaib, S. (2021). Selection of tumor-resistant variants following sustained natural killer cell-mediated immune stress. *Oncology Reports*, *45*(2), 582-594. https://doi.org/10.3892/or.2020.7872

Chiang, A.-J., Li, C.-J., Tsui, K.-H., Chang, C., Chang, Y. I., Chen, L.-W., Chang, T.-H., & Sheu, J. J.-C. (2021). UBE2C Drives Human Cervical Cancer Progression and Is Positively Modulated by mTOR. *Biomolecules*, *11*(1), 37. https://doi.org/10.3390/biom11010037

Chou, S.-M., Yen, Y.-H., Yuan, F., Zhang, S.-C., & Chong, C.-M. (2023). Neuronal Senescence in the Aged Brain. *Aging and Disease*, *14*(5), 1618-1632. https://doi.org/10.14336/AD.2023.0214

Davalli, P., Mitic, T., Caporali, A., Lauriola, A., & D'Arca, D. (2016). ROS, Cell Senescence, and Novel Molecular Mechanisms in Aging and Age-Related Diseases. *Oxidative Medicine and Cellular Longevity*, *2016*, 3565127. https://doi.org/10.1155/2016/3565127

Feles, S., Overath, C., Reichardt, S., Diegeler, S., Schmitz, C., Kronenberg, J., Baumstark-Khan, C., Hemmersbach, R., Hellweg, C. E., & Liemersdorf, C. (2022). Streamlining Culture Conditions for the Neuroblastoma Cell Line SH-SY5Y: A Prerequisite for Functional Studies. *Methods and Protocols*, *5*(4), 58. https://doi.org/10.3390/mps5040058

Gan, Y., Ye, F., & He, X.-X. (2020). The role of YWHAZ in cancer: A maze of opportunities and challenges. *Journal of Cancer*, *11*(8), 2252-2264. https://doi.org/10.7150/jca.41316

Gao, Y.-F., Zhu, T., Chen, J., Liu, L., & Ouyang, R. (2018). Knockdown of collagen α-1(III) inhibits glioma cell proliferation and migration and is regulated by miR128-3p. *Oncology Letters*, *16*(2), 1917-1923. https://doi.org/10.3892/ol.2018.8830

Haigis, M. C., & Yankner, B. A. (2010). The Aging Stress Response. *Molecular Cell*, *40*(2), 333-344. https://doi.org/10.1016/j.molcel.2010.10.002

Hamazaki, J., & Murata, S. (2024). Relationships between protein degradation, cellular senescence, and organismal aging. *The Journal of Biochemistry*, *175*(5), 473-480. https://doi.org/10.1093/jb/mvae016

Hernandez-Segura, A., Nehme, J., & Demaria, M. (2018). Hallmarks of Cellular Senescence. *Trends in Cell Biology*, *28*(6), 436-453. https://doi.org/10.1016/j.tcb.2018.02.001

Hou, Y., Dan, X., Babbar, M., Wei, Y., Hasselbalch, S. G., Croteau, D. L., & Bohr, V. A. (2019). Ageing as a risk factor for neurodegenerative disease. *Nature Reviews. Neurology*, *15*(10), 565-581. https://doi.org/10.1038/s41582-019-0244-7

Huang, S., & Li, X. (2024). UBE2C promotes LUAD progression by ubiquitin-dependent degradation of p53 to inactivate the p53/p21 signaling pathway. *Discover Oncology*, *15*(1), 589. https://doi.org/10.1007/s12672-024-01465-4

Jia, Y.-J., Wang, J., Ren, J.-R., Chan, P., Chen, S., Chen, X.-C., Chhetri, J. K., Guo, J., Guo, Q., Jin, L., Liu, Q., Liu, Q., Ma, W., Mao, Z., Song, M., Song, W., Tang, Y., Wang, D., Wang, P., … Pei, G. (2023). A framework of biomarkers for brain aging: A consensus statement by the Aging Biomarker Consortium. *Life Medicine*, *2*(3), lnad017. https://doi.org/10.1093/lifemedi/lnad017

Kim, Y.-J., Lee, G., Han, J., Song, K., Choi, J.-S., Choi, Y.-L., & Shin, Y. K. (2020). UBE2C Overexpression Aggravates Patient Outcome by Promoting Estrogen-Dependent/Independent Cell Proliferation in Early Hormone Receptor-Positive and HER2-Negative Breast Cancer. *Frontiers in Oncology*, *9*. https://doi.org/10.3389/fonc.2019.01574

Kondo, T., Oue, N., Yoshida, K., Mitani, Y., Naka, K., Nakayama, H., & Yasui, W. (2004). Expression of POT1 is Associated with Tumor Stage and Telomere Length in Gastric Carcinoma. *Cancer Research*, *64*(2), 523-529. https://doi.org/10.1158/0008-5472.CAN-03-1196

Kovalevich, J., & Langford, D. (2013). Considerations for the Use of SH-SY5Y Neuroblastoma Cells in Neurobiology. *Methods in molecular biology (Clifton, N.J.)*, *1078*, 9-21. https://doi.org/10.1007/978-1-62703-640-5_2

Kuivaniemi, H., & Tromp, G. (2019). Type III collagen (COL3A1): Gene and protein structure, tissue distribution, and associated diseases. *Gene*, *707*, 151-171. https://doi.org/10.1016/j.gene.2019.05.003

Kuleshov, M. V., Jones, M. R., Rouillard, A. D., Fernandez, N. F., Duan, Q., Wang, Z., Koplev, S., Jenkins, S. L., Jagodnik, K. M., Lachmann, A., McDermott, M. G., Monteiro, C. D., Gundersen, G. W., & Ma'ayan, A. (2016). Enrichr: A comprehensive gene set enrichment analysis web server 2016 update. *Nucleic Acids Research*, *44*(Web Server issue), W90-W97. https://doi.org/10.1093/nar/gkw377

Kumari, R., & Jat, P. (2021). Mechanisms of Cellular Senescence: Cell Cycle Arrest and Senescence Associated Secretory Phenotype. *Frontiers in Cell and Developmental Biology*, *9*. https://doi.org/10.3389/fcell.2021.645593

Laoukili, J., Kooistra, M. R. H., Brás, A., Kauw, J., Kerkhoven, R. M., Morrison, A., Clevers, H., & Medema, R. H. (2005). FoxM1 is required for execution of the mitotic programme and chromosome stability. *Nature Cell Biology*, *7*(2), 126-136. https://doi.org/10.1038/ncb1217

Laoukili, J., Stahl, M., & Medema, R. H. (2007). FoxM1: At the crossroads of ageing and cancer. *Biochimica Et Biophysica Acta*, *1775*(1), 92-102. https://doi.org/10.1016/j.bbcan.2006.08.006

Laresgoiti, U., Apraiz, A., Olea, M., Mitxelena, J., Osinalde, N., Rodriguez, J. A., Fullaondo, A., & Zubiaga, A. M. (2013). E2F2 and CREB cooperatively regulate transcriptional activity of cell cycle genes. *Nucleic Acids Research*, *41*(22), 10185-10198. https://doi.org/10.1093/nar/gkt821

Lee, N. Y. S., Li, M., Ang, K. S., & Chen, J. (2023). Establishing a human bone marrow single cell reference atlas to study ageing and diseases. *Frontiers in Immunology*, *14*, 1127879. https://doi.org/10.3389/fimmu.2023.1127879

Li, R., Teng, Y., Guo, Y., Ren, J., Li, R., Luo, H., Chen, D., Feng, Z., Fu, Z., Zou, X., Wang, W., & Zhou, C. (2023). Aging-related decrease of histone methyltransferase SUV39H1 in adipose-derived stem cells enhanced SASP. *Mechanisms of Ageing and Development*, *215*, 111868. https://doi.org/10.1016/j.mad.2023.111868

Liu, H., Chen, L., Xiao, W., Liu, J., Long, C., Zhan, W., Cui, C., Yang, L., & Chen, S. (2022). Alteration of E2F2 Expression in Governing Endothelial Cell Senescence. *Genes*, *13*(9), 1522. https://doi.org/10.3390/genes13091522

López-Otín, C., Blasco, M. A., Partridge, L., Serrano, M., & Kroemer, G. (2023). Hallmarks of aging: An expanding universe. *Cell*, *186*(2), 243-278. https://doi.org/10.1016/j.cell.2022.11.001

Macedo, J. C., Vaz, S., Bakker, B., Ribeiro, R., Bakker, P. L., Escandell, J. M., Ferreira, M. G., Medema, R., Foijer, F., & Logarinho, E. (2018). FoxM1 repression during human aging leads to mitotic decline and aneuploidy-driven full senescence. *Nature Communications*, *9*(1), 2834. https://doi.org/10.1038/s41467-018-05258-6

Mazumder, B., Sampath, P., Seshadri, V., Maitra, R. K., DiCorleto, P. E., & Fox, P. L. (2003). Regulated Release of L13a from the 60S Ribosomal Subunit as A Mechanism of Transcript-Specific Translational Control. *Cell*, *115*(2), 187-198. https://doi.org/10.1016/s0092-8674(03)00773-6

Nishimura, Y., Komatsu, S., Ichikawa, D., Nagata, H., Hirajima, S., Takeshita, H., Kawaguchi, T., Arita, T., Konishi, H., Kashimoto, K., Shiozaki, A., Fujiwara, H., Okamoto, K., Tsuda, H., & Otsuji, E. (2013). Overexpression of YWHAZ relates to tumor cell proliferation and malignant outcome of gastric carcinoma. *British Journal of Cancer*, *108*(6), 1324-1331. https://doi.org/10.1038/bjc.2013.65

Peters, A. H. F. M., O'Carroll, D., Scherthan, H., Mechtler, K., Sauer, S., Schöfer, C., Weipoltshammer, K., Pagani, M., Lachner, M., Kohlmaier, A., Opravil, S., Doyle, M., Sibilia, M., & Jenuwein, T. (2001). Loss of the Suv39h Histone Methyltransferases Impairs Mammalian Heterochromatin and Genome Stability. *Cell*, *107*(3), 323-337. https://doi.org/10.1016/S0092-8674(01)00542-6

Pinzaru, A. M., Hom, R. A., Beal, A., Phillips, A. F., Ni, E., Cardozo, T., Nair, N., Choi, J., Wuttke, D. S., Sfeir, A., & Denchi, E. L. (2016). Telomere Replication Stress Induced by POT1 Inactivation Accelerates Tumorigenesis. *Cell reports*, *15*(10), 2170-2184. https://doi.org/10.1016/j.celrep.2016.05.008

Poddar, D., Basu, A., Baldwin, W., Kondratov, R. V., Barik, S., & Mazumder, B. (2013). An extra-ribosomal function of ribosomal protein L13a in macrophage resolves inflammation. *Journal of immunology (Baltimore, Md. : 1950)*, *190*(7), 3600-3612. https://doi.org/10.4049/jimmunol.1201933

Ridderinkhof, K. R., & Krugers, H. J. (2022). Horizons in Human Aging Neuroscience: From Normal Neural Aging to Mental (Fr)Agility. *Frontiers in Human Neuroscience*, *16*. https://doi.org/10.3389/fnhum.2022.815759

Rong, N., Mistriotis, P., Wang, X., Tseropoulos, G., Rajabian, N., Zhang, Y., Wang, J., Liu, S., & Andreadis, S. T. (2019). Restoring extracellular matrix synthesis in senescent stem cells. *The FASEB Journal*, *33*(10), 10954-10965. https://doi.org/10.1096/fj.201900377R

Sidler, C., Woycicki, R., Li, D., Wang, B., Kovalchuk, I., & Kovalchuk, O. (2014). A role for SUV39H1-mediated H3K9 trimethylation in the control of genome stability and senescence in WI38 human diploid lung fibroblasts. *Aging (Albany NY)*, *6*(7), 545-563. https://doi.org/10.18632/aging.100678

Statzer, C., Park, J. Y. C., & Ewald, C. Y. (2023). Extracellular Matrix Dynamics as an Emerging yet Understudied Hallmark of Aging and Longevity. *Aging and Disease*, *14*(3), 670-693. https://doi.org/10.14336/AD.2022.1116

Takai, H., Jenkinson, E., Kabir, S., Babul-Hirji, R., Najm-Tehrani, N., Chitayat, D. A., Crow, Y. J., & de Lange, T. (2016). A POT1 mutation implicates defective telomere end fill-in and telomere truncations in Coats plus. *Genes & Development*, *30*(7), 812-826. https://doi.org/10.1101/gad.276873.115

von Zglinicki, T. (2024). Oxidative stress and cell senescence as drivers of ageing: Chicken and egg. *Ageing Research Reviews*, *102*, 102558. https://doi.org/10.1016/j.arr.2024.102558

Wang, W., Zhang, L., Wang, Y., Ding, Y., Chen, T., Wang, Y., Wang, H., Li, Y., Duan, K., Chen, S., Yang, Q., & Chen, C. (2017). Involvement of miR-451 in resistance to paclitaxel by regulating YWHAZ in breast cancer. *Cell Death & Disease*, *8*(10), e3071. https://doi.org/10.1038/cddis.2017.460

Wu, Z., Qu, J., Zhang, W., & Liu, G.-H. (2024). Stress, epigenetics, and aging: Unraveling the intricate crosstalk. *Molecular Cell*, *84*(1), 34-54. https://doi.org/10.1016/j.molcel.2023.10.006

Xicoy, H., Wieringa, B., & Martens, G. J. M. (2017). The SH-SY5Y cell line in Parkinson's disease research: A systematic review. *Molecular Neurodegeneration*, *12*, 10. https://doi.org/10.1186/s13024-017-0149-0

Yates, L. A., Zhang, X., & Burgers, P. M. (2025). DNA Damage and Replication Stress Checkpoints. *Annual Review of Biochemistry*, *94*, 195-221. https://doi.org/10.1146/annurev-biochem-072324-031915

Zade, N. H., & Khattar, E. (2023). POT1 mutations cause differential effects on telomere length leading to opposing disease phenotypes. *Journal of Cellular Physiology*, *238*(6), 1237-1255. https://doi.org/10.1002/jcp.31034

Zhang, M. J., Pisco, A. O., Darmanis, S., & Zou, J. (t.y.). Mouse aging cell atlas analysis reveals global and cell type-specific aging signatures. *eLife*, *10*, e62293. https://doi.org/10.7554/eLife.62293

8. SUPPLEMENTARY MATERIAL

Gene Name	Forward Primer Sequence	Reverse Primer Sequence	Annealing Temperature (°C)	Efficiency (%)
HPRT1	5'-TGACACTGGCAAAACAATGCA-3'	5'-GGTCCTTTTCACCAGCAAGCT-3'	59.50	99.31%
YWHAZ	5'-ACTTTTGGTACATTGTGGCTTCAA-3'	5'-CCGCCAGGACAAACCAGTAT-3'	59.50	98.72%
RPL13A	5'-CCTGGAGGAGAAGAGGAAAGAGA-3'	5'-TTGAGGACCTCTGTGTATTTGTCAA-3'	59.50	103.74%
COL3A1	5'-CGATGAGATTATGACTTC-3'	5'-ATTACAGAATACCTTGATAG-3'	53.00	107.44%
UBE2C	5'-ACATATGCCTGGACATCCTGA-3'	5'-GGTTCTCCTAGAAGGCTCTGG-3'	59.50	98.46%
FOXM1	5'-ACTTTAAGCACATTGCCAAGC-3'	5'-CGTGCAGGGAAAGGTTGT-3'	55.90	100.90%
E2F2	5'-CCAAGAATTACATCAGAGAA-3'	5'-GCTTACATTCCAGACTTC-3	55.90	96.06%
SUV39H1	5'-CTACTATGGCAACATCTC-3'	5'-GTCAAGGTTGTCTATGAA-3'	55.90	86.30%
POT1	5'-GAAGTGGACGGAGCATCATT-3'	5'-TTTGTAGCCGATGGATGTGA-3'	55.00	99.27%

Supplementary Table S1. *Primer sequences, annealing temperatures, and amplification efficiencies for the candidate genes analyzed by qPCR.*